Original scientific paper

Informacije MIDEM
Journal of Microelectronics,
Electronic Components and Materials
Vol. 47, No. 3(2017), 165 – 170

Multicaloric effect in polycrystalline $Pb(Fe_{0.5}Nb_{0.5})O_3$

Uros Prah[1,2], Magdalena Wencka[3], Zdravko Kutnjak[1, 2], Marko Vrabelj[1], Silvo Drnovsek[1], Barbara Malic[1, 2] and Hana Ursic[1,2]

[1]*Jožef Stefan Institute, Ljubljana, Slovenia*
[2]*Jožef Stefan International Postgraduate School, Ljubljana, Slovenia*
[3]*Institute of Molecular Physics, Polish Academy of Sciences, Poznań, Poland*

Abstract: In this work, magnetocaloric and electrocaloric properties of multiferroic $Pb(Fe_{0.5}Nb_{0.5})O_3$ ceramics have been investigated. $Pb(Fe_{0.5}Nb_{0.5})O_3$ was prepared by mechanochemical activation of constituent oxides, followed by sintering at 1273 K in oxygen atmosphere. Microstructure and X-ray powder-diffraction analysis revealed dense, homogeneous and uniform microstructure without the presence of undesired secondary phases. Magnetocaloric and electrocaloric effects were determined by the indirect methods - calculated from the changes of sample's magnetization and polarization, respectively. The maximal magnetocaloric temperature change (0.16 K at 50 kOe) was obtained at 2 K coinciding with the observed anomaly in magnetization vs. temperature measurement. On the other hand, at room temperature the pronounced electrocaloric effect was determined, namely 0.81 K at 80 kV/cm, while the maximal value of electrocaloric temperature change 1.29 K was obtained near the paraelectric-ferroelectric phase transition i.e., at 373 K.

Keywords: multiferroic; PFN; multicaloric; electrocaloric; magnetocaloric

Multikalorčni pojav v polikristaliničnem $Pb(Fe_{0.5}Nb_{0.5})O_3$

Izvleček: V članku smo proučevali magnetokalorični in elektrokalorični pojav v multiferoičnem $Pb(Fe_{0.5}Nb_{0.5})O_3$. Keramiko smo pripravili z mehanokemijsko aktivacijo kovinskih oksidov, ki ji je sledilo sintranje pri 1273 K v kisikovi atmosferi. Mikrostruktura keramike je bila gosta in homogena. Sekundarnih faz nismo opazili. Tako magnetokalorično kot tudi elektrokalorično temperaturno spremembo smo izračunali iz temperaturne spremembe magnetizacije oz. polarizacije vzorca pri različnih zunanjih poljih. Največjo magnetokalorično spremembo temperature (0,16 K pri 50 kOe) smo določili pri 2 K, kar je v skladu z opaženo anomalijo magnetizacije vzorca v odvisnosti od temperature. Izrazito elektrokalorično spremembo temperature smo opazili že pri sobni temperaturi (0,81 K pri 80 kV/cm), medtem ko je bila njena maksimalna vrednost 1,29 K opažena v bližini paraelektričnega-feroelektričnega faznega prehoda pri 373 K.

Ključne besede: multiferoik; PFN; multikalorik; elektrokalorik; magnetokalorik

** Corresponding Author's e-mail: uros.prah@ijs.si*

1 Introduction

Nowadays the majority of commercially used refrigeration systems are still based on vapor-compression refrigeration cycle. This technology was discovered at the beginning of the 19th century and has been developed and perfected through the years. Despite all the improvements, the method shows a number of disadvantages. The major problems are low energy efficiency and the use of environmentally hazardous refrigerant media [1, 2]. These disadvantages has driven the development of more efficient and environmentally friendly cooling devices.

Solid-state refrigeration technology represents a promising alternative for the replacement of the conventional refrigeration systems. Most current activity in cooling research is looking at one of the caloric effects – magnetocaloric (MC), electrocaloric (EC) or mechanocaloric – where the material's entropy changes under the application of external stimuli –magnetic, electric, or mechanical (stress) [3]. However, in bulk ceramic materials the caloric effect is currently not large enough for commercial use. One idea how to overcome this problem is to prepare a material exhibiting more than one caloric effect, called multicaloric material, in which

the application of two or more stimuli can enhance the total caloric effect. Further, different caloric modes can be applied in different temperature regions extending the operating temperature range of the cooling device [4].

In 2012, the coexistence of the MC and EC effects in a single-phase material was theoretically introduced for the first time [5]. In the next years, many theoretical reports were followed [6-8]. In 2014, a multicaloric effect in Y_2CoMnO_6 was experimentally observed [9]. However, this material exhibit improper multiferroic properties and therefore the conventional methods for determining the EC effect are not appropriate. In 2016 the existence of multicaloric properties in $0.8Pb(Fe_{0.5}Nb_{0.5})O_3$–$0.2Pb(Mg_{0.5}W_{0.5})O_3$ (PFN-20PMW) ceramic material was demonstrated, where the coexistence of MC and EC effects was unequivocally experimentally confirmed [4]. While PFN-20PMW appears promising, it possesses very small MC and EC temperature changes (both ~0.25 K). Further, the largest caloric effects in this material are observed at low temperatures of 5 K (MC) and 220 K (EC), which is far too low for any practical applications.

One of the more promising candidates is multiferroic $Pb(Fe_{0.5}Nb_{0.5})O_3$ (PFN) ceramic. It possesses a relatively high peak of the dielectric permittivity (several 10,000) at around 370 K, which is attributed to the paraelectric-ferroelectric phase transition [10]. Because the highest caloric effects are obtained near ferroic phase transitions [11, 12], PFN should possess high EC properties above the room temperature. On the other hand, in this material two anomalies are reported also in the temperature dependence of the magnetic susceptibility. These two anomalies appear at 150 K and 10 K [13, 14] indicating a potential for enhanced MC effect close to these temperatures.

One possibility of preparing complex oxides is the use of mechanochemical synthesis, where homogeneous powders can be prepared without thermal treatment. Later the powder compacts are sintered at elevate temperature (T > 1200 K) to obtain dense ceramics. It was shown that $(K_{0.485}Na_{0.485}Li_{0.03})(Nb_{0.8}Ta_{0.2})O_3$ and $Pb(Sc_{0.5}Nb_{0.5})O_3$ ceramics prepared from the mechanochemically synthesized powders have exhibited superior chemical homogeneity in comparison to the one prepared by the classical solid-state synthesis [15, 16]. PFN has already been prepared with a mechanochemical synthesis [17-19] and in comparison to the solid-state synthesized samples, it possesses higher values of peak-permittivity, which can be presumably attributed to the better chemical homogeneity of the former one [15]. In this work we prepared a single-phase PFN ceramic by mechanochemical synthesis and sintering aiming to study its dielectric, electrocaloric and magnetocaloric properties.

2 Experimental

For the synthesis of the PFN powder, Nb_2O_5 (99.9%, Sigma-Aldrich, 208515), Fe_2O_3 (99.9%, Alfa, 014680-Ventron) and PbO (99.9%, Sigma-Aldrich, 211907) were used. The homogenized stoichiometric mixture (200 g) was mechanochemically activated in a high-energy planetary ball mill (Retsch, Model PM 400) for 30 h at 300 rpm using a tungsten carbide milling vial (250 cm^3) and 15 balls (2r = 20 mm). The synthesized powder was milled in an attrition mill with yttria-stabilized zirconia balls (2r = 3 mm) in isopropanol, for 4 h at 800 rpm.

The powder was then uniaxially pressed (50 MPa) into pellets and further consolidated by isostatic pressing at 300 MPa. The powder compacts were sintered in double alumina crucibles in the presence of a packing powder with the same chemical composition, in order to avoid possible PbO losses. The compacts were sintered at 1273 K for 2 h in an oxygen atmosphere with the heating and cooling rates of 2 K/min.

The density of the sintered pellets was determined with Archimedes' method. For the calculation of relative density, the theoretical density of 8.46 g/cm^3 was used (PDF card no. 032-0522).

The X-ray powder-diffraction (XRD) of the PFN powder after the mechanochemical treatment and crushed sintered pellet were recorded using a PANalytical X'Pert PRO (PANalytical, Almelo, Netherlands) diffractometer with Cu-$K\alpha_1$ radiation. The XRD patterns were collected over the 2θ range 10–70°, with a step of 0.034° and 100 s per step.

For the microstructural analysis the samples were fractured for fracture-surface examination, ground and polished using standard metallographic techniques for polish-surface examination and thermally etched at 1023 K for 20 min and fine polishing (by a colloidal silica suspension with 0.04 μm sized colloidal SiO_2 particles for 1.5 h) for thermally etched-surface examination. The microstructure was studied with a field-emission scanning electron microscope (FE-SEM, JSM-7600F JEOL Ltd., Japan) at 15 kV with a working distance of 15 mm. The grain size and their distribution were determined from the micrographs of the thermally etched samples, where more than 340 grains per sample were measured using the Image Tool Software [20]. The grain size is expressed as the Feret's diameter [21].

For the dielectric measurements, the pellets were cut and thinned to a thickness of about 200 µm and then the Cr/Au electrodes (2r = 5 mm) were sputtered on samples' surfaces. The dielectric permittivity (ε´) at different temperatures was measured with a HP 4284 A Precision LCR impedance meter in the temperature range from 298 K to 473 K.

The EC effect was determined by the indirect method; the EC temperature change (ΔT_{EC}) was calculated from the polarization versus electric field (*P–E*) measured by Aixacct TF analyzer 2000 (Aixacct, Aachen, Germany) at 10 Hz in a temperature range between 298 and 363 K (step 5 K). For the calculation of ΔT_{EC}, the equation given in ref. [22] was used.

The MC effect was determined by the indirect method; the MC temperature change (ΔT_{MC}) was calculated from the magnetization (*M*) versus temperature measurements at different magnetic fields (1–50 kOe) using a Superconducting Quantum Interference Device magnetometer in a temperature range from 2 to 350 K. The mass of the sample was 30 mg. For the calculation of ΔT_{MC}, the equation given in ref. [23] was used.

The specific heat capacity (C_p), which was needed for the calculation of ΔT_{EC} and ΔT_{MC} was measured on a 30 mg cube-shaped sample in a temperature range between 2 and 393 K using Physical Property Measurement System.

3 Results

The XRD patterns of the PFN powder and crushed pellets are shown in Fig. 1. All the peaks correspond to the perovskite phase (PDF card no. 032-0522) and no secondary phases were observed. Broader diffraction peaks and higher background in the case of powder can be attributed to smaller size of the crystallites and the presence of the amorphous phase, as suggested in [24] for $Pb(Mg_{0.33}Nb_{0.67})O_3$. The density of the ceramic was 8.1 g/cm^3, which is equal to 95.7% of the theoretical density.

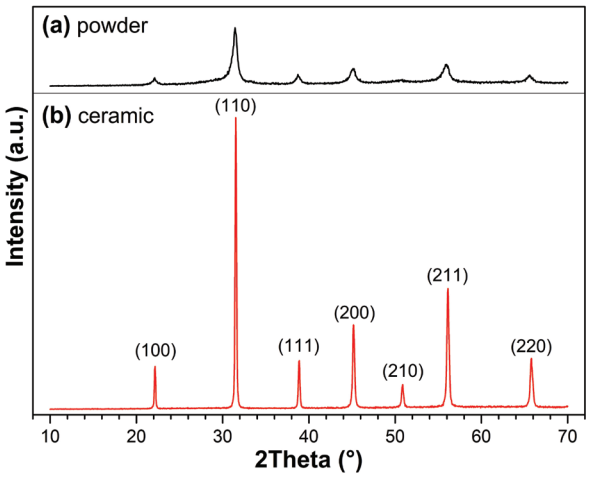

Figure 1: XRD patterns of (a) the PFN powder and (b) crushed pellet.

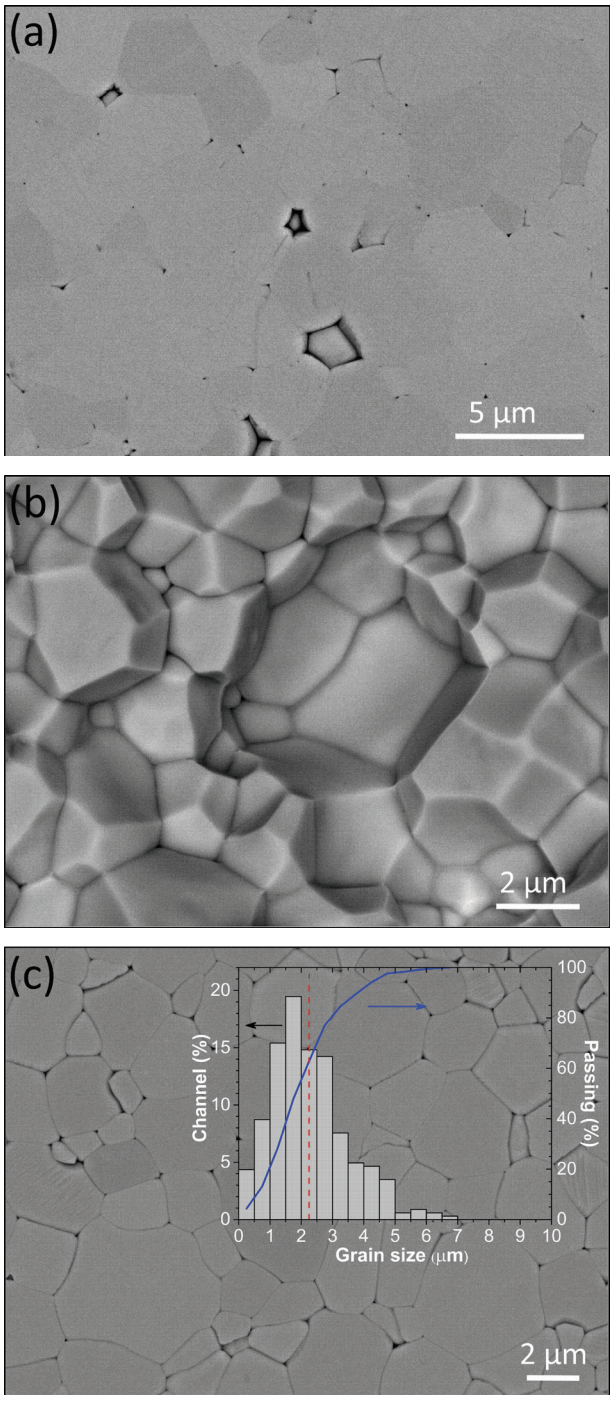

Figure 2: (a) Polished, (b) fractured and (c) thermally etched FE-SEM images. Inset: the grain size distribution with the cumulative curve.

The FE-SEM micrographs of the polished, fractured and thermally etched surfaces (Figs. 2a-c) of PFN ceramic reveal dense, homogeneous and uniform microstructures with the average grain size of (2.3 ± 1.2) μm and unimodal grain size distribution (inset on Fig. 2c). No secondary phases were detected with the FE-SEM analysis in agreement with the XRD analysis.

The temperature dependence of ε' is shown in Fig. 3. The value at room temperature (298 K) and 1 kHz is 3780. The maximal value of permittivity (ε'_{max}) at 1 kHz is ~28200 and it just slightly decreases with increasing frequency (~27200 at 100 kHz). The measured ε'_{max} value is higher than previously reported one for solid-state synthesized PFN [25, 26] and comparable with the one for ceramics prepared by mechanochemical synthesis [19].

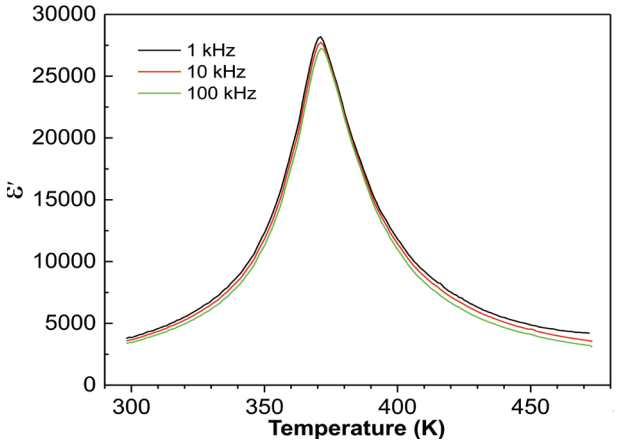

Figure 3: Temperature dependence of ε′.

As shown in Fig. 3 the peak-permittivity temperature (T_m) is at 371 K (for all frequencies), which is in agreement with the previously reported ones [26, 27]. According to the literature, this anomaly of ε′ indicates a paraelectric-ferroelectric phase transition [28, 29].

P–E hysteresis loops at different temperatures are shown in Fig. 4a. At room temperature (298 K), typical ferroelectric hysteresis loop is observed. The values of the remanent polarization (P_r), maximum polarization (P_{max}) and coercive field (E_c) at room temperature are ~22.5 μAs/cm², ~41.6 μAs/cm² and ~4.4 kV/cm, respectively. The P_r and P_{max} values decreased with the increasing temperature (i.e., P_r ~ 9.1 μAs/cm² and P_{max} ~ 35.1 μAs/cm² at 363 K).

The temperature dependence of ΔT_{EC} is shown in Fig. 4b. The ΔT_{EC} at room temperature and 80 kV/cm is 0.81 K. The ΔT_{EC} increases with the increasing temperature and increasing applied electric field. The maximum ΔT_{EC} of 1.29 K was obtained at 80 kV/cm and 373 K.

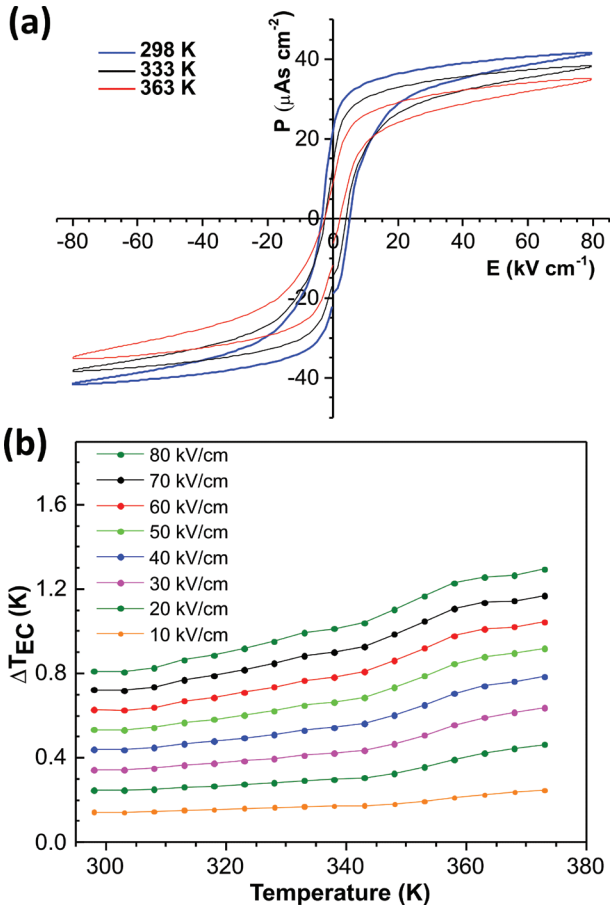

Figure 4: (a) *P–E* hysteresis loops and (b) ΔT_{EC} versus temperature.

The temperature dependence of *M* at different magnetic fields is shown in Fig. 5a. The *M* increases with increasing magnetic field and decreasing temperature, therefore the highest value of 1.37 Am²/kg was observed at 2 K and 50 kOe. Two anomalies are observed in *M* (*T*, *H*) curves in accordance with the literature [14, 15]. The one at ~150 K is attributed to the paramagnetic-antiferromagnetic phase transition, while the second one at ~10 K to antiferromagnetic-antiferromagnetic phase transition.

The temperature dependence of ΔT_{MC} is shown in Fig. 5b. The ΔT_{MC} at room temperature and 50 kOe is very low, i.e., ~2 mK. The ΔT_{MC} increases with the decreasing temperature (in proportion to magnetization) and increasing applied magnetic field, therefore the maximum ΔT_{MC} of 0.16 K was obtained at 50 kOe and 2 K.

4 Summary and conclusions

In this work, we were able to prepare single-phase PFN ceramics showing both EC and MC properties. The ce-

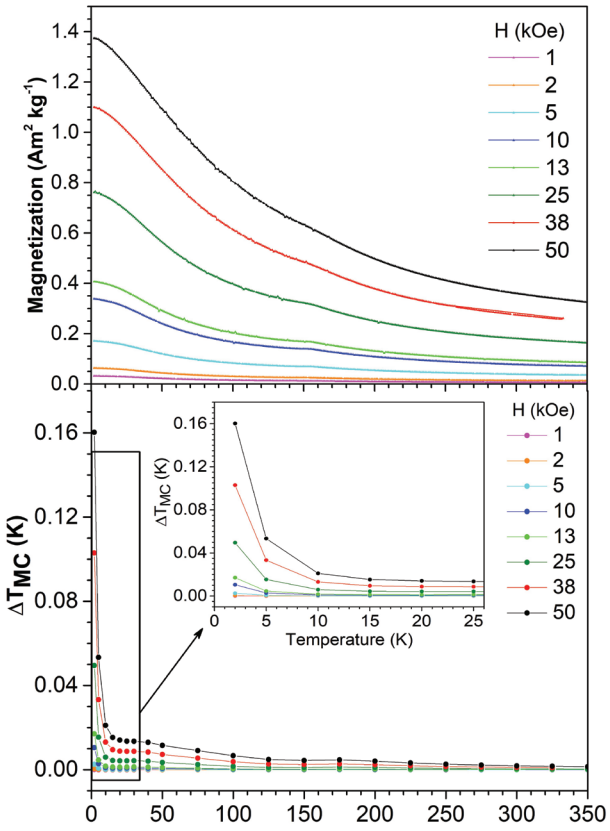

Figure 5: (a) *M* and (b) ΔT_{MC} versus temperature.

ramic pellets were prepared by mechanochemical synthesis of the constituent oxides and thermal treatment at 1237 K. Microstructure analysis revealed dense, homogeneous and uniform microstructures with the average grain size of ~2.3 μm. At room temperature and 1 kHz the value of ε' was 3780.

The highest value of magnetization (i.e., 1.37 Am^2/kg) was measured at low temperature of 2 K. At this temperature also the maximum ΔT_{MC} ~ 0.16 K was determined. On the other hand, the ΔT_{EC} reaches the value as high as 1.29 K at 373 K. But even at room temperature the ΔT_{EC} was relatively high, i.e., 0.81 K. Further work is needed in order to confirm EC properties by direct EC temperature measurements, for example by high-resolution calorimetry.

5 Acknowledgments

The authors would like to thank the Slovenian Research Agency (research core funding no. P2-0105 and project PR-07594) and joint research project between Polish and Slovenian Academy of Sciences "*Multicaloric relaxor materials for new cooling technologies*".

6 References

1. M. Ozbolt, A. Kitanovski, J. Tusek, A. Poredos, "Electrocaloric vs. magnetocaloric energy conversion," Int. J. Refrig. 37, pp. 16–27, 2014.
2. T. Correia, Q. Zhang, Eds., Electrocaloric materials: New Generation of Coolers, 1st ed. Berlin, Heidelberg, Germany: Springer-Verlag Berlin Heidelberg, 2014.
3. X. Moya, S. Kar-Narayan, N. D. Mathur, "Caloric materials near ferroic phase transition," Nat. Mater. 13, pp. 439–450, 2014.
4. H. Ursic, V. Bobnar, B. Malic, C. Filipic, M. Vrabelj, S. Drnovsek, Y. Jo, M. Wencka, Z. Kutnjak, "A multicaloric material as a link between electrocaloric and magnetocaloric refrigeration," Sci. Rep. 6, pp. 26629 1–5, 2016.
5. M. M. Vopson, "The multicaloric effect in multiferroic materials," Solid State Commun. 152, pp. 2067–2070, 2012.
6. A. Kumar, K. L. Yadav, "Study on multicaloric effect of CuO induced multiferroic," J. Appl. Phys. 116, pp. 083907 1–3, 2014.
7. A. Planes, T. Castan, A. Saxena, "Thermodynamics of multicaloric effects in multiferroics," Philos. Mag. 94, pp. 1893–1908, 2014.
8. A. S. Starkov, I. A. Starkov, "Multicaloric Effect in a Solid: New Aspects," J. Exp. Theor. Phys. 119, pp. 258–263, 2014.
9. J. K. Murthy, A. Venimadhav, "Multicaloric effect in multiferroic Y_2CoMnO_6," J. Phys. D: Appl. Phys. 47, pp. 445002 1–6, 2014.
10. V. V. Bhat, K.V. Ramanujachary, S. E. Lofland, A. M. Umarji, "Tuning the multiferroic properties of $Pb(Fe_{1/2}Nb_{1/2})O_3$ by cationic substitution," J. Magn. Magn. Mater. 280, pp. 221–226, 2004.
11. X. Moya, S. Kar-Narayan, N. D. Mathur, "Caloric materials near ferroic phase transitions," Nat. Mater. 13, pp. 439–450, 2014.
12. B. Rozic, M. Kosec, H. Ursic, J. Holc, B. Malic, Q. M. Zhang, R. Blinc, R. Pirc and Z. Kutnjak, "Influence of the critical point on the electrocaloric response of relaxor ferroelectrics," J. Appl. Phys. 110, pp. 064118 1–5, 2011.
13. R. Havlicek, J. Poltierova Vejppravova, D. Bochenek, "Structure and magnetic properties of perovskite-like multiferroic $PbFe_{0.5}Nb_{0.5}O_3$," J. Phys. Conf. Ser. 200, pp. 012058 1–4, 2009.
14. S. Matteppanavar, B. Angadi, S. Rayaprol, "Low temperature magnetic studies on $PbFe_{0.5}Nb_{0.5}O_3$ multiferroic," Physica B: Condensed Matter 448, pp. 229–232, 2014.
15. T. Rojac, A. Bencan, M. Kosec, "Mechanism and Role of Mechanochemical Activation in the Synthesis of $(K,Na,Li)(Nb,Ta)O_3$Ceramisc," J. Am. Ceram. Soc., 93, pp. 1619–1625, 2010.

16. H. Ursic, A. Bencan, G. Drazic, G. Esteves, J. L. Jones, T.-M. Usher, T. Rojac, S. Drnovsek, M. Deluca, J. Jouin, V. Bobnar, G. Trefalt, J. Holc, B. Malic, "Unusual structural-disorder stability of mechanochemically derived-Pb($Sc_{0.5}Nb_{0.5}$)O_3," J. Mater. Chem. C, 3, pp. 10309–10315, 2015.
17. X. Gao, J. Xue, J. Wang, "Sequential Combination of Constituent Oxides in the Synthesis of Pb($Fe_{1/2}Nb_{1/2}$)O_3 by Mechanical Activation," J. Am. Ceram. Soc. 85, pp. 565–572, 2002.
18. A. A. Gusev, I. P. Raevski, E. G. Avvakumov, V. P. Isupov, S. I. Raevskaya, H. Chen, V. V. Titov, C.-C. Chou, S. P. Kubrin, S. V. Titov, M. A. Malitskaya, "Dielectric Properties of Undopedand Li-doped Pb($Fe_{1/2}Nb_{1/2}$)O_3 Ceramics Sintered from Mechanochemically Synthesized Powders," Ferroelectrics 475, pp. 61–67, 2015.
19. R. Mackeviciute, V. Goian, S. Greicius, R. Grigalaitis, D. Nuzhnyy, J. Holc, J. Banys, S. Kamba, "Lattice dynamics and broad-band dielectric properties of multiferroic Pb($Fe_{1/2}Nb_{1/2}$)O_3 ceramics," J. Appl. Phys. 117, pp. 084101 1–6, 2015.
20. D. Wilcox, B. Dove, B. McDavid, D. Greer, "UTHSCSA Image Tool for Windows version 3.0." University of Texas Health Science Center, San Antonio, 2002.
21. W. H. Walton, "Feret`s statistical diameter as a measure of particle size," Nature, 162, pp. 329–330, 1948.
22. Z. Kutnjak, B. Rozic, R. Pirc, Electrocaloric effect: theory, measurements, and applications, Wiley Encyclopedia of Electrical and Electronics Engineering, John Wiley & Sons, Inc., New Jersey, 2015.
23. A. Kitanovski, J. Tusek, U. Tomc, U. Plaznik, M. Ozbolt, A. Poredos, Magnetocaloric energy convertion, ISSN 1865-3529, Springer International Publishing Switzerland, Switzerland, 2015.
24. D. Kuscer, J. Holc, M. Kosec, "Mechano-Synthesis of Lead-Magnesium-Niobate Ceramics," J. Am. Ceram. Soc. 89, pp. 3081–3088, 2006.
25. R. Font, O. Raymond-Herrera, L. Mestres, J. Portelles, J. Fuentes, J. M. Siqueiros, "Improvement of the dielectric and ferroelectric properties of multiferroic Pb($Fe_{1/2}Nb_{1/2}$)O_3 ceramics processed in oxygen atmosphere," J. Mater. Sci. 51, pp. 6319–6330, 2016.
26. C. C. Chiu, S. B. Desu, "Microstructure and properties of lead ferroniobate ceramics (Pb($Fe_{0.5}Nb_{0.5}$)O_3)," Mater. Sci. Eng., B21, pp. 26–35, 1993.
27. R. Sun, W. Tan, B. Fang, "Perovskite phase formation and electrical properties of Pb($Fe_{1/2}Nb_{1/2}$)O_3 ferroelectric ceramicse," Phys. Status Solidi A, 206, pp. 326–331, 2009.
28. M. Yokosuka, "Electrical and Electromechanical Properties of Hot-Pressed Pb($Fe_{1/2}Nb_{1/2}$)O_3 Ferroelectric Ceramics," Jpn. J. Appl. Phys. 32, pp. 1142–1146, 1993.
29. X. S. Gao, X. Y. Chen, J. Yin, J. Wu, Z. G. Liu, "Ferroelectric and dielectric properties of ferroelectromagnet Pb($Fe_{1/2}Nb_{1/2}$)O_3 ceramics and thin films," J. Mater. Sci. 35, pp. 5421–425, 2000.

Arrived: 31. 08. 2017
Accepted: 07. 11. 2017